Loss of TRIM21 drives UVB-induced systemic inflammation by regulating DNA-sensing pathways

Gantsetseg Tumurkhuu[1,2], Richard Moore[1,2], Graziela Perri[1,2], Gabriela de los Santos[1,2], Duygu Ercan Laguna[1,2], David Gibb[2,3], Jessica Carriere[2,3], Christian Stehlik[2,3], Caroline A. Jefferies[1,2]
[1]Kao Autoimmunity Institute, Division of Rheumatology, Department of Medicine, Cedars-Sinai Medical Center, Los Angeles, California; [2]Department of Biomedical Sciences, Cedars-Sinai Medical Center, Los Angeles, California; [3]Department of Pathology and Laboratory Medicine; Cedars-Sinai Medical Center, Los Angeles, California

ABSTRACT

Background. Patients with systemic lupus erythematosus (SLE) experience photosensitivity, with exposure to ultraviolet light B (UVB) driving lupus flares and triggering symptoms like joint pain, fatigue, and cutaneous lesions. Although the mechanism(s) linking UVB exposure to systemic effects are unclear, type I interferons (IFNs) are known to play a role. Our previous work has shown that TRIM21, an autoantigen in SLE, functions as a negative regulator on the pathways driving IFN expression. Here we explore how TRIM21 functions to regulate both local and systemic inflammation following UVB exposure and that altered expression may drive cutaneous inflammation and photosensitivity in SLE.

Methods. WT (C57BL/6) and *Trim21*$^{-/-}$ mice were irradiated with UVB (100mJ/cm^2) on shaved dorsal region of the mice on consecutive days for 1 and 3 weeks, and UVB induced local cutaneous manifestations and systemic inflammation in blood, spleen and kidney were examined by messenger RNA expression of inflammatory and type I IFN response genes, histology, and flow cytometry. To determine the molecular targets of TRIM21 downstream of UVB, mechanistic studies were performed in bone marrow-derived macrophages (BMDMs) and mouse skin fibroblasts (MDF) from WT and *Trim21*$^{-/-}$ mice, and *TRIM21*$^{-/-}$ THP-1 cells.

Results. Infiltration of inflammatory cells and induction of type I IFN developed in UVB-exposed areas in both sets of mice. Most notably after UVB exposure, we observed splenomegaly and enhanced expression of IFN-stimulated genes (ISG) in the blood and spleen of *Trim21*$^{-/-}$ mice. Subsequent analysis showed higher expression of Siglec1, an IFN-inducible protein, on Ly6C^{hi} inflammatory monocytes in the spleen and blood cells of UVB-exposed *Trim21*$^{-/-}$ mice, indicating a systemic IFN response. Inflammatory chemokines CXCL10 and CXCL12, both important in UVB-induced skin inflammation, were also detected at significantly higher levels in serum of *Trim21*$^{-/-}$ mice after UVB exposure. In addition, *Trim21*$^{-/-}$ mice exposed to UVB also demonstrated enhanced total IgG levels in serum accompanied by increased skin deposition of IgG. Altogether, loss of *Trim21* in mice results in enhanced systemic IFN-driven responses and mimics increased systemic disease in SLE patients following UVB exposure. TRIM21 acts to restrain RNA/DNA sensing and IFN responses, and enhanced basal and UVB- and cGAMP-dependent *Ifnb1* expression was observed in *Trim21*$^{-/-}$ BMDMs and MDFs. In cells obtained from *Trim21/Sting1* double knockout mice, cGAMP and cytoplasmic dsDNA induced *Ifnb1* expression was reduced, indicating that TRIM21 regulates *Ifnb1* expression through the adaptor protein STING. As TRIM21 is an E3 ligase and known to regulate protein stability, we assessed protein levels of cGAS, DDX41 and STING itself. Mechanistically, we found both degradation of DDX41 and STING levels were affected in stimulated *Trim21*$^{-/-}$ BMDMs. Taken together, our results indicate that TRIM21 protects against IFN induction at local and systemic levels due to a failure to restrict STING signaling. Understanding the role of TRIM21 in preventing systemic disease will have important understandings of its role in driving increased disease activity and flare in SLE.

Introduction

Abnormal responses to ultraviolet B (UVB) light or photosensitivity are experienced by approximately two thirds of systemic lupus erythematosus (SLE) patients, with sun-exposure triggering either local skin inflammation, increased systemic activity (flare), or both (1). The mechanisms that predispose patients to develop systemic disease flares in response to sun exposure are unclear and are an important gap in our knowledge regarding the pathophysiology of this disease. Elevated type I interferon (IFNα, β and κ) and IFN-stimulated genes (ISG) are the most common immunologic abnormality in SLE and associate with disease severity and organ involvement, including cutaneous involvement (2-5). Photosensitivity to UVB is a well-known trigger of both localized cutaneous disease (CLE) and systemic disease. In cutaneous manifestations of SLE, high levels of type I IFNs are detected in both lesional and non-lesional skin and correlate with systemic ISG expression (6). UVB exposure has multiple effects on keratinocytes, the first line of defense against exposure, including IFN induction (2, 7). However, the molecular links between UVB-photosensitivity and development of systemic disease are unknown.

Mechanistically, UVB exposure triggers several biologic pathways in the skin including DNA damage, DNA repair, cell death, and release of self-nucleic acids. Self-RNA and DNA (mitochondrial and nucleic) act as potent damage-associated molecular patterns (DAMPs), and are detected by cytosolic nucleic acid sensors (5, 8-12) such as cGAS and DDX41 (13-15). cGAS, once it binds dsDNA, synthesizes the cyclic dinucleotide cyclic-GMP-AMP (cGAMP) which acts as a second messenger in the cell, binding and activating the adaptor protein STING to drive IFNβ induction (16-19). DDX41 can also bind cGAMP and STING and drive IFNβ expression (13, 14). Recent work has clearly implicated cGAS and STING in UVB-mediated IFN expression in the skin of C57BL/6 mice, with the absence of STING or cGAS preventing IFN induction in the skin following UVB exposure (20, 21).

TRIM21, otherwise known as Ro52, is a common autoantigen associated with cutaneous SLE and is commonly upregulated in photo-provoked skin (7). Moreover, anti-Ro52/TRIM21 antibodies accumulate in CLE skin and exacerbate local inflammatory responses. As an E3 ubiquitin ligase TRIM21 negatively regulates type I IFN induction downstream of RNA and DNA sensing pathways by ubiquitinating and targeting DDX41 and the transcription factors IRF3, 5 and 7 for proteosomal degradation (22-30). In doing so, TRIM21 limits the IFN response and prevents autoimmune disease. *Trim21*-deficient mice develop splenomegaly and a lupus-like systemic disease as a result of enhanced TLR7 and 9-induced IFN induction, driven by increased levels of IRF3, 5 and 7 (27). Importantly *Trim21*$^{-/-}$ mice exhibit skin lesions that are provoked by DNA damage, suggesting *Trim21* may play an important role in skin-involvement in SLE (27).

In this study we explored the potential that loss of *Trim21* might exacerbate UVB-induced skin and systemic inflammation. We found *Trim21*-deficiency results in enhanced local and systemic inflammation and ISG expression of UVB-exposed mice. In addition to increased DDX41 stability, we observed *Trim21*$^{-/-}$ cells fail to degrade STING after engaging the cGAS/STING pathway, resulting in upregulated type I IFN and ISGs. Our findings show that TRIM21 is an important regulator of systemic IFN responses following UVB challenge in the skin and suggest that loss of TRIM21 expression or activity in the skin of SLE patients with cutaneous involvement may enhance UVB-induced systemic involvement.

Materials and Methods

Mice

Trim21$^{GFP/GFP}$ mice (*Trim21*$^{-/-}$) were a gift from the Dr. Wahren-Herlenius lab (27). C57BL/6 and *Sting*^{gt} mice were purchased from The Jackson Laboratory. Mice were propagated and maintained in the animal facility at the Department of Comparative Medicine (Davis Building) of Cedars-Sinai Medical Center. Animals were between 8-12 weeks old at the time of experimentation. All experiments procedure was approved by institutional IACUC committee.

UVB irradiation regime

Eight-week-old wild-type (WT) and *Trim21*$^{-/-}$ were shaved dorsally prior to UVB exposure. Mice were allowed to move freely in their cage during UVB exposure and mice were treated with/without UVB 100 mJ/cm^2 for one or three weeks.

Isolation of skin, spleen cells and flow cytometry

Skin lesion, spleen, and blood were harvested following final UVB exposure. To generate a single cell suspension, spleens were passed through a 70-µM filter. Skin samples were minced and digested with 0.28 units/ml Liberase TM (Roche) and 0.1 mg/ml of Deoxyribonuclease I (Worthington) for 60 minutes at 37°C, then passed through a 70-µM filter and washed with 1% bovine serum albumin in phosphate buffered saline. Cells were then incubated in flow block (1% bovine serum albumin and 1% horse serum in PBS) for 30 min, followed by staining with mouse-specific fluorescent antibodies CD45 Alexa Fluor 700 (clone:30-F11), CD3 PE/Cy7 (clone 145-2C11), CD4 APC/Cy7 (clone GK1.5), CD11b Pacific Blue (clone M1/70), Ly6G APC (clone 1A8), CCR2 PE (clone SA203G11), all purchased from BioLegend (San Diego, CA); Siglec1 BV421 (clone 7-239) (BD Bioscience) for 45 minutes. All samples were processed using SA3800 flow cytometer (Sony) and data analyzed with FlowJo VX.0.7 software (Tree Star).

Analysis of anti-IgG and dsDNA IgG antibody serum levels. Serum was collected post UVB treatment. Total IgG and anti-dsDNA IgG antibody levels were analyzed via ELISA kits (6320 and 5120, Alpha Diagnostic, San Antonio, TX).

Histopathology, immunohistochemistry, and immunofluorescence

Tissue samples were immersed in 10% buffered formalin for 48 hours at 4°C, paraffin embedded, and stained using hematoxylin and eosin. For immunofluorescence, following the addition of secondary antibodies, slides were stained with DAPI, washed, air-dried, and mounted. Images were taken on a Zeiss Axio Observer and anti-IgG intensity was quantified using ImageJ.

Isolation, culture, and stimulation of cells and tissue

Bone marrow-derived macrophages (BMDMs) were cultured as previously described (31). Briefly, bone marrow was flushed from the tibia and femurs of 8-10 week old mice and differentiated for 7 days in DMEM supplemented with 10% fetal bovine serum (FBS, Omega Scientific Inc), 1X Gibco Antibiotic-Antimycotic (A/A, 15240062, Thermo Fisher Scientific), and 20% L929-conditioned media in a 37°C, 5% CO_2 incubator.

Murine dermal fibroblasts (MDFs) and skin explants were cultured as previously described (32). Briefly, mice were euthanized and shaved dorsal skin was excised and digested with collagenase D and pronase. MDFs were cultured in RPMI-1640 Medium (11875119, ThermoFisher Scientific) supplemented with 10% FBS and 1X A/A. Skin explant assay was performed as previously described (33). Briefly, explants were excised from shaved dorsal skin of euthanized mice using 6-mm punch biopsies and cultured similarly to MDFs. Before

stimulation, MDFs and skin explants were starved in 2% FBS-supplemented medium for 24 hours before exposure to 50, 100, or 500 mJ/cm^2 UVB.

50 nM immunostimulatory dsDNA (ISD) was transfected into BMDMs or THP-1 cells with Lipofectamine (L3000008, ThermoFisher Scientific) for 1, 2, 4, or 8 hours. 2'-3-cyclic GMP-AMP (cGAMP) (tlrl-nacga23-1, InvivoGen) was added at 10 µg/mL with or without 4µM H151 (inh-h151, InvivoGen) to cell supernatant (added 30 minutes prior to stimulation) for 1, 2, 4, or 8 hours.

Generation of *TRIM21*$^{-/-}$ and THP-1 cells and *TRIM21* knock-in of *TRIM21*$^{-/-}$ THP-1 cells

TRIM21$^{-/-}$ THP-1 cells were generated using CRISPR/Cas9 targeting. Two guide RNAs (gRNAs) were designed to target hTRIM21 Exon 2: gRNA#1: ATGCTCACAGGCTCCACGAA (Exon2 ORF bp67-86); gRNA#2: ATGTTGGCTAGCTGTCGATT (Exon2 ORF bp196-215) and cloned into lentiCRISPRv1 (Addgene, plasmid 49535). After lentiviral transduction using lentiCRISPRv1 as control as described below, clonal populations were screened by PCR amplification and sequencing of the targeted genomic sequence using the following primers: hTrim21gRNA1-Fwd: GTCTCCACACTGCTGTTTAACG; hTrim21gRNA2-Rev: TTCCCATCTTTCTCACAGAACA. To restore *TRIM21* expression into *TRIM21*$^{-/-}$ THP-1 cells, hTRIM21 full-length CDS with N-terminal Myc and EGFP was cloned into pLEX-MCS and transfected into HEK293T-Lenti cells (Clontech 632180) along with pMD.2G and psPAX2 (Addgene, plasmids 12259 and 12260) to generate lentiviral particles. Forty-eight hours post-transfection, lentiviral suspensions were harvested, passed through 0.45µm filters and mixed with 106 TRIM21KO THP-1 cells in the presence of 0.5µg/mL polybrene. Cells were centrifuged at 1,800rpm for 50min at 32°C. After overnight incubation at 37°C, the medium was changed and EGFP$^+$ cells were sorted 72h post-infection.

Western Blot

Cells were lysed after ISD transfection or cGAMP stimulation using RIPA lysis buffer (0.05% SDS, 0.5% NP-40, and 0.25% Na-Deoxycholate in PBS) and quantified using BCA Protein Assay Kit (ThermoFisher Scientific). 20 µg sample per lane were loaded onto 4-20% precast polyacrylamide gel membrane and then transferred onto nitrocellulose membranes (BioRad). Membranes were labeled with anti-DDX41 (Novus Bio), anti-IRF3 (clone D83B9, Cell Signaling Technology), anti-STING (Novus Bio), anti-TRIM21 (clone EPR20290, abcam), and anti-β-actin (Cell Signaling Technology). Following incubation with HRP-conjugated anti-mouse or anti-rabbit IgG (Cell Signaling Technology), signals were visualized with SuperSignal West Pico PUS Chemiluminescent Substrate (ThermoFisher Scientific) on a ChemiDoc XRS+ Scanner (BioRad).

Gene expression analysis

RNA was isolated from full-thickness skin samples using RNeasy Fibrous Tissue Mini Kit with on-column DNase treatment (Qiagen). From whole blood, splenocytes, and in vitro cells, RNA was isolated using TRI Reagent (Millipore Sigma). First-strand complementary DNA (cDNA) was generated using 500 ng RNA with a High-Capacity cDNA Reverse Transcription Kit using random primers (Applied Biosystems). Reactions were run in triplicate on a StepOnePlus real-time PCR instrument (Applied Biosystems) using gene-specific primers. Ct values were standardized to the house-keeping gene *Rn18s* (mouse) or *RNA18SN* (human).

The following murine primer sequences were used: *Rn18s*, 5′-GAGGGAGCCTGAGAAACGG-3′ (forward) and 5′-GTCGGGAGTGGGTAATTTGC-3′ (reverse); *Cxcl10*, 5′-GCCGTCATTTTCTGCCTCAT-3′ (forward) and 5′-GCTTCCCTATGGCCCTCATT-3′ (reverse); for *Ifnb1*, 5'-CAGCTCCAAGAAAGGACGAAC-3' (forward) and 5'-

GGCAGTGTAACTCTTCTGCAT-3’ (reverse); *Isg15*, 5’-GGTGTCCGTGACTAACTCCAT-3’ (forward) and 5’-TGGAAAGGGTAAGACCGTCCT-3’ (reverse). The following human primer sequences were used: RNA18SN, 5’- -3’ (forward), 5’- -3’ (reverse); *IFNB1*, 5’-CTTGGATTCCTACAAAGAAGCAGC-3’ (forward) and 5’- TCCTCCTTCTGGAACTGCTGCA-3’ (reverse).

STATISTICS

All data was graphed, and statistics performed using GraphPad Prism. For data comparing multiple groups, two-Way ANOVA with Fisher’s LSD test was used. Comparison between two groups was completed via a two-tailed Student's t-test for normally distributed data. Comparisons were considered significant with a p value of <0.05.

Results

The loss of TRIM21 accelerates UVB induced cutaneous inflammation. Ultraviolet B (UVB) and C (UVC) light drive type I IFN in keratinocytes, and both acute and repeated UVB exposure result in upregulation of type I IFN and IFN-stimulated genes (ISGs) within the skin of mice (34). Mice lacking TRIM21 develop severe dermatitis and systemic autoimmunity in response to chronic physical injury (27). To test whether TRIM21 plays a role in regulating the IFN-response to chronic UVB exposure, we shaved *Trim21*$^{+/+}$ (WT) and *Trim21*$^{-/-}$ (KO) C57BL/6 mice and exposed them to a low dose of UVB light on consecutive days over three weeks. While both WT and *Trim21*$^{-/-}$ animals demonstrated similar levels of infiltrating CD45^{+} immune cells into the skin following chronic UVB exposure (Supplementary Figure 1), CD11b^{+} cells were increased in UVB-exposed *Trim21*$^{-/-}$ skin (Figure 1A) and had higher levels of the IFN-stimulated gene (ISG), Siglec1, compared to WT CD11b^{+} cells (Figure 1B). In addition, IFNβ and the IFN-stimulated gene *Cxcl10* were significantly upregulated in *Trim21*-deficient skin tissue compared to WT (Figure 1C), with skin from *Trim21*-deficient animals showed significantly higher deposition of IgG in the skin after UVB compared to WT (Figure 1D).

Loss of *Trim21* enhances the Systemic Inflammatory Response to UVB. In addition to the local immune response, acute UVB exposure also induces inflammation of the spleen and kidney (35). Because of this, we asked if Trim21 protected against systemic inflammation due to chronic UVB exposure. We observed enhanced splenomegaly in *Trim21*$^{-/-}$ mice compared to WT (Figure 2A) with higher total levels of CD11b^{+} cells in the spleens of *Trim21*$^{-/-}$ mice (supplemental figure 1b). In addition, whilst splenic levels of CD11b^{+}Ly6G^{+} cells increased in mice exposed to UVB spleens of *Trim21*$^{-/-}$ mice had significantly higher levels compared to spleens from WT (Figure 2B). In keeping with enhanced IFN responses, CD11b^{+} splenic populations from *Trim21*$^{-/-}$ mice had increased expression of the IFN-inducible marker Siglec1 compared to WT mice (Figure 2C). In addition, expression of *IFNβ* and *Mx1* was also enhanced in the spleens of UVB exposed *Trim21*$^{-/-}$ mice (Figure 2D). Noticeably, the percentage of CD4+ T cells in the spleen increased in the absence of *Trim21* (Figure 2E), with central memory CD4 T cells being more highly represented in the spleens of *Trim21*$^{-/-}$ mice compared to WT controls (Figure 2F) than did UVB-exposed WT mice.

It has been previously shown that circulating CCR2^{+} monocytes are upregulated in response to UVB exposure and migrate to the UVB-exposed tissue to drive inflammation (21). In line with this, we observed that increased CD11b+Ly6G+ circulating neutrophils and inflammatory monocytes (CD11b+Ly6C+) in UVB-exposed *Trim21*$^{-/-}$ mice compared to WT controls (Figure 3A) and that the total percentage of CCR2+CD11b+ myeloid cells were increased compared to WT controls (Figure 3B) and expressed higher levels of the IFN-stimulated gene Siglec1 (Figure 3C). In addition, *Trim21*$^{-/-}$ mice had higher circulating IgG compared to WT (Figure 3D), although no increase in anti-dsDNA IgG was observed following three weeks of UVB exposure (data not shown). Altogether, these data support that loss of Trim21 exacerbates the systemic inflammatory response to UVB exposure.

TRIM21 Restricts the IFN-I Response via STING Signaling

The cGAS-STING pathway has recently been shown to regulate UVB-induced systemic responses in mice (21, 35, 36). In addition DDX41 has previously been shown to be a target for TRI21-mediated ubiquitination and degradation. To assess the effect of TRIM21-deficiency on DDX41 and STING stability, we stimulated BMDMs from WT and *Trim21*$^{-/-}$ mice with immunostimulatory dsDNA (ISD) which activates cGAS upstream of STING and analyzed DDX41 and STING stability by western blotting. As previously published, DDX41 and STING were degraded in a time-dependent manner following transfection of WT BMDMs with ISD

(Figure 4A, left-hand panel). In contrast, both DDX41 and STING were stabilized in *Trim21*$^{-/-}$ mice (Figure 4A, right-hand panel), which was mirrored by enhanced IFNβ expression in TRIM21-deficient BMDMs stimulated with either ISD or the STING ligand cGAMP (Figure 4B, left and right-hand panel, respectively). We next confirmed these results in THP1 cells in which TRIM21 had been knocked down using CRISPR-Cas9 targeting, followed by reconstitution of these TRIM21-deficient THP1s with wild-type TRIM21 (as shown in Supplemental Figure 3A). Knockdown of TRIM21 resulted in enhanced IFNβ expression in response to ISD transfection compared to control THP1 cells, which was reversed following lentiviral introduction of TRIM21-EGP into the cells (Supplemental Figure 3B). Analysis of DDX41 and STING by western blotting in these cell lines confirmed the role of TRIM21 as a critical regulator of their stability – with TRIM21-containing THP1 inducing DDX41 and STING degradation in response to ISD transfection, whereas loss of TRIM21 prevented STING and DDX41 degradation (Supplemental Figure 3C). We next asked whether the increased type I IFN response we observed in the skin and systemically in *Trim21*$^{-/-}$ mice in response to UVB exposure was dependent on STING signaling. Primary murine dermal fibroblasts (MDFs) from WT or *Trim21*$^{-/-}$ mice were UVB-treated with or without H151, a STING specific inhibitor (37), and assessed for IFNβ expression by qPCR. In keeping with our in vivo studies, MDFs from *Trim21*$^{-/-}$ mice showed enhanced UVB-induced IFNβ expression compared to MDFs from WT mice, with H151 substantially reducing UVB-driven IFN responses in *Trim21*$^{-/-}$ MDFs (Figure 4C). Similarly, bone marrow derived macrophages (BMDMs) from WT and *Trim21*$^{-/-}$ mice showed enhanced IFNβ expression in response to the secondary messenger and STING cGAMP, that was reduced in both WT and *Trim21*$^{-/-}$ BMDMs by coincubation with H151 (Figure 4D). BMDMs from *Trim21*$^{-/-}$ mice crossed with *Sting*$^{gt/gt}$ mice showed reduced IFNβ expression compared to *Trim21*$^{-/-}$ BMDMs alone when stimulated with either cGAMP or transfected with ISD (Figure 4E). Finally, we cultured skin explants from WT, *Trim21*$^{-/-}$ and *Trim21*$^{-/-}$*Sting*$^{gt/gt}$ mice ex vivo and UVB irradiated them with 500mJ/cm^2 for 24 hours. qPCR analysis of skin explants from each genotype demonstrated that whilst *Trim21*$^{-/-}$ explants exhibited higher *Ifnb1* and *Isg15* expression than did explants from WT mice, and the absence of *Sting* reversed these effects (Figure 4F).

Figure 5: Given the protective effect of TRIM21 on UVB-driven responses in mice, we next assessed whether there was any alteration in TRIM21 expression in SLE patients with cutaneous LE (CLE). Intriguingly, we found that TRIM21 levels were significantly lower in patients with CLE, suggesting that loss of TRIM21 expression may contribute to photosensitivity in SLE. Based on these findings we hypothesize that TRIM21 protects against photosensitivity in SLE by regulating cytosolic nucleic acid sensing pathways in response to UVB stimulation. Thus, in summary, our data demonstrates that UVB irradiation of murine skin drives IFNβ and ISG expression both locally and systemically in a STING-dependent manner, and that the absence of *Trim21* results in exacerbated responses both locally and systemically. Our data strongly suggests that TRIM21 acts as a gatekeeper to restrain IFN responses to cytosolic DNA, potentially as a result of its ability to degrade DDX41.

Discussion

TRIM21 is an important autoantigen associated with cutaneous SLE and is also a critical negative regulator of type I IFN induction in response to RNA and DNA sensing. UVB is an important environmental trigger for both cutaneous SLE and in driving systemic flares, and has recently been shown in mice to activate both local and systemic type I IFN responses via a cGAS-STING dependent pathway. As loss of *Trim21* has previously been shown to result in skin inflammation we hypothesized that mice deficient in *Trim21* may be hypersensitive to UVB exposure. In keeping with this, we observed that *TRIM21*-deficient mice developed splenomegaly and systemic induction of type I IFNs in response to chronic UVB exposure compared to WT mice. This was accompanied by increased numbers of neutrophils and inflammatory monocytes, both in the circulation and in the spleen, and that this corresponded with increased expression of CCR2, a chemokine receptor critical for homing to inflamed tissues (such as the kidney or spleen). In addition, central memory CD4+ T cells were also increased in Trim21-deficient mice exposed to chronic low doses of UVB, suggesting that loss of *Trim21* results in enhanced CD4 T cell activation. Assessing potential targets for TRIM21 in this model revealed that the DNA sensor DDX41 and STING protein levels were stable in *Trim21*$^{-/-}$ murine cells, whereas both were decreased in a time-dependent manner in response to UVB or ISD transfection in cells derived from WT mice. Importantly, enhanced expression of *Ifnβ* in *Trim21*$^{-/-}$ MDFs and BMDMs could be rescued by inhibiting signaling through STING, either through loss of *Tmem173* or using a STING-specific inhibitor. Importantly we observe decreased expression of TRIM21 in whole blood samples from SLE patients with cutaneous involvement, in addition to decreased expression of TRIM21 in the lesional skin of patients with cutaneous SLE compared to non-lesional skin. Our data underlines the importance of TRIM21 as a negative regulator of type I IFN responses and suggests that in the context of UVB-driven responses in SLE, loss of TRIM21 expression or activity may promote UVB-induced SLE exacerbations.

UV irradiation causes damage in cells via direct DNA damage leading to formation of pyrimidine dimers and activation of the DNA damage response via p53 activation. Indirect DNA damage results from oxidative stress and production of reactive oxygen species (ROS), driving oxidation of bases such as 8-oxo-2'-deoxyguanoisine (8-OH-dG) and single-stranded DNA breaks (16,17 of review). Indeed, we have previously shown that loss of Ogg1 in mice, an enzyme that degrades 8-OH-dG, develops a lupus-like disease and enhanced responses to pristane induced SLE, accompanied by increased expression of type I IFNs (Tumurkhuu G et al., 2020). In SLE, UVB exposure is accompanied by type I IFN and CXCL10 induction and are important in the pathogenesis of cutaneous involvement in SLE (3,39,42). In our studies, absence of Trim21 results in exacerbated IFNβ and CXCL10 in the skin following UVB exposure, indicating that Trim21 negatively regulates the production of these cytokines. In addition, we observe enhanced recruitment of CD45+ immune cells, and more importantly enhanced levels of expression of Siglec1, an IFN stimulated gene, on CD11b+ cells, indicating enhanced exposure of these cells to type I IFN.

The role of type I IFNs in cutaneous manifestations of SLE is well established, with production of type I IFN by epidermal cells and Langerhans cells responsible for priming inflammatory and apoptotic responses in the skin (2, 7, 38, 39). Recent single cell transcriptomic profiling of cells from lesional and non-lesional skin from SLE patients with active cutaneous involvement identified an overall high IFN-rich signature in both lesional and non-lesional skin, suggesting that normal appearing skin in SLE patients is actually primed immunologically and exists in a prelesional state (6). Another important implication from this analysis was that non classical monocytes in the periphery may be the source of the abundant levels of CD16^{+} dendritic cells observed in both lesional and non-lesional skin. These findings suggest that changes in the skin

microenvironment promote immune cell infiltration and skewing towards pathogenic subtypes. In line with this, recent murine studies have shown that the transition from skin to systemic inflammation requires cGAS-STING signaling and that neutrophil and monocyte recruitment to inflamed skin in UVB models requires IFN signaling. Indeed, in the absence of cGAS the monocyte chemoattractant CCL2 (MCP-1) is diminished (36). Thus in early responses to UVB, both CCL2 and IFN are required for neutrophil and monocyte recruitment to the skin. In our study we observe that systemic effects in response to skin exposure to UVB are exacerbated in *Trim21*$^{-/-}$ mice and that increased expression of Siglec1, an IFN-inducible gene, is observed on circulating CD11b^{+} cells. In addition, inflammatory CD11b^{+}Ly6C^{+} monocytes show increased expression of the chemokine receptor *Ccr2*, the receptor for CCL2, which is required to home cells to inflamed tissues, including the skin and kidneys (1, 21, 35, 36, 40).

UVB also induces rapid accumulation of neutrophils to the skin in murine models . In the absence of *Trim21*, no differences in neutrophil numbers in the skin following UVB exposure compared to WT are observed. However, an increase in both relative percentage and absolute numbers of neutrophils in the blood and spleen of UVB-exposed *Trim21*$^{-/-}$ mice were seen. This is in keeping with a recent study that examined the kinetics of neutrophil recruitment to the skin in C57BL/6 mice exposed acutely to UVB (35). In this study the authors observed that neutrophils trafficked to the skin within 24 hours post-UVB exposure and remained there for up to 6 days. This was accompanied by an increase in neutrophils systemically and in the spleen, in accordance with our own findings. This study also showed that neutrophils that accumulated in the skin in response to UVB, and trafficked to the kidney in a CXCR4-Cxcl12 dependent manner to drive kidney inflammation and that blocking IL-17A or G-CSF could ameliorate these effects (35). In our study we observed enhanced IFN-stimulated gene expression in the kidneys of *Trim21*$^{-/-}$ mice exposed to UVB. However, other markers of UVB-induced kidney damage such as ICAM-1, lipocalin and S100A9 were not altered however. Interestingly, the original characterization of the Trim21$^{-/-}$ mice used in this study also found that SLE-like responses and skin lesions that developed spontaneously in the *Trim21*$^{-/-}$ mice and that blocking IL23 mediated IL17A expression could reverse this phenotype (27). Therefore our observations suggest that exacerbated systemic inflammation in response to UVB-exposure of the skin in Trim21-/- mice may be as a result of enhance IL-23/IL-17A signaling and neutrophil accumulation in affected organs.

While TRIM21 is an important autoantigen in SLE and Sjogren's disease, its role in the pathobiology of SLE and Sjogren's has been somewhat ambiguous. As an autoantigen it has been shown to be extruded on blebs of apoptosing keratinocytes in response to UVB irradiation – thus promoting autoantibody formation. It is also an IFN regulated gene, thus its expression is frequently increased in SLE peripheral immune cells. However given its known role in downregulating IFN responses in response to nucleic acid sensing, its increased expression in SLE should be associated with enhanced down regulation of nucleic acid sensing via its ability to target DDX41 and the transcription factors IRF3, 5 and 7. However, in SLE enhanced levels of expression of these transcription factors, consistent with loss of function of TRIM21 in these cells. Recently the discovery of different isoforms of TRIM21 has provided a potential explanation for this apparent anomaly. TRIM21α is the full length form of the enzyme, complete with RING-B-Box-Coiled-Coil(CC)-SPRY/PRY domains. The RING domain interacts with the E3 ligase machinery, the B-Box and CC domains are important for homo-dimerization and the SPRY/PRY domain interacts with the target to be ubiquitinated (ie IRF3, 5 and 7). TRIM21γ has recently been described as a short-form isoform, missing the SPRY/PRY domain. We and others have shown that loss of the SPRY/PRY domain results in TRIM21$^{\Delta SPRY/PRY}$ acting as a dominant negative and thereby preventing down-regulation of nucleic acid (NA)-induced IFN induction (refs). We have also shown that the SPRY/PRY domain is phosphorylated in its active

site and promotes binding to IRF3 and potentially other substrates. Therefore the increased expression of TRIM21/Ro52γ in SLE neutrophils and myeloid cells described by Gomez-(41) E et al. , may contribute to altered function of full-length TRIM21 in SLE. Consistent with this, we observe that loss of the SPRY/PRY domain prevents TRIM21-dependent inhibition of ISD or cGAMP-induced IFNβ expression in THP1 cells, in addition to stabilized DDX41, indicating that in the absence of the SPRY/PRY domain TRIM21 is no longer able to degrade its substrates, in keeping with our previous observations. However the exact nature of isoform-specific function of TRIM21 in regulating NA sensing pathways in the context of SLE remains to be elucidated.

References

1. Kuechle MK, Elkon KB. Shining light on lupus and UV. Arthritis Res Ther. 2007;9(1):101.
2. Sarkar MK, Hile GA, Tsoi LC, Xing X, Liu J, Liang Y, et al. Photosensitivity and type I IFN responses in cutaneous lupus are driven by epidermal-derived interferon kappa. Ann Rheum Dis. 2018;77(11):1653-64.
3. Ronnblom L, Leonard D. Interferon pathway in SLE: one key to unlocking the mystery of the disease. Lupus Sci Med. 2019;6(1):e000270.
4. Ronnblom LE, Alm GV, Oberg KE. Possible induction of systemic lupus erythematosus by interferon-alpha treatment in a patient with a malignant carcinoid tumour. J Intern Med. 1990;227(3):207-10.
5. Gunther C. Nucleic Acid Immunity in the Pathogenesis of Cutaneous Lupus Erythematosus. Front Immunol. 2019;10:1636.
6. Billi AC, Ma F, Plazyo O, Gharaee-Kermani M, Wasikowski R, Hile GA, et al. Nonlesional lupus skin contributes to inflammatory education of myeloid cells and primes for cutaneous inflammation. Science translational medicine. 2022;14(642):eabn2263.
7. Stannard JN, Reed TJ, Myers E, Lowe L, Sarkar MK, Xing X, et al. Lupus Skin Is Primed for IL-6 Inflammatory Responses through a Keratinocyte-Mediated Autocrine Type I Interferon Loop. J Invest Dermatol. 2017;137(1):115-22.
8. Svobodova AR, Galandakova A, Sianska J, Dolezal D, Lichnovska R, Ulrichova J, Vostalova J. DNA damage after acute exposure of mice skin to physiological doses of UVB and UVA light. Arch Dermatol Res. 2012;304(5):407-12.
9. Collison J. Faulty mitochondrial DNA repair promotes inflammation in RA. Nat Rev Rheumatol. 2019;15(10):576.
10. Barber GN. STING-dependent cytosolic DNA sensing pathways. Trends in immunology. 2014;35(2):88-93.

11. Hagiwara AM, Moore RE, Wallace DJ, Ishimori M, Jefferies CA. Regulation of cGAS-STING pathway - Implications for systemic lupus erythematosus %J Rheumatology and Immunology Research. 2021;2(3):173-84.
12. McWhirter SM, Jefferies CA. Nucleic Acid Sensors as Therapeutic Targets for Human Disease. Immunity. 2020;53(1):78-97.
13. Parvatiyar K, Zhang Z, Teles RM, Ouyang S, Jiang Y, Iyer SS, et al. The helicase DDX41 recognizes the bacterial secondary messengers cyclic di-GMP and cyclic di-AMP to activate a type I interferon immune response. Nat Immunol. 2012;13(12):1155-61.
14. Zhang Z, Yuan B, Bao M, Lu N, Kim T, Liu YJ. The helicase DDX41 senses intracellular DNA mediated by the adaptor STING in dendritic cells. Nat Immunol. 2011;12(10):959-65.
15. Sun L, Wu J, Du F, Chen X, Chen ZJ. Cyclic GMP-AMP synthase is a cytosolic DNA sensor that activates the type I interferon pathway. Science. 2013;339(6121):786-91.
16. Ablasser A, Goldeck M, Cavlar T, Deimling T, Witte G, Rohl I, et al. cGAS produces a 2'-5'-linked cyclic dinucleotide second messenger that activates STING. Nature. 2013;498(7454):380-4.
17. Gao D, Wu J, Wu YT, Du F, Aroh C, Yan N, et al. Cyclic GMP-AMP synthase is an innate immune sensor of HIV and other retroviruses. Science. 2013;341(6148):903-6.
18. Wu J, Sun L, Chen X, Du F, Shi H, Chen C, Chen ZJ. Cyclic GMP-AMP is an endogenous second messenger in innate immune signaling by cytosolic DNA. Science. 2013;339(6121):826-30.
19. Diner EJ, Burdette DL, Wilson SC, Monroe KM, Kellenberger CA, Hyodo M, et al. The innate immune DNA sensor cGAS produces a noncanonical cyclic dinucleotide that activates human STING. Cell Rep. 2013;3(5):1355-61.
20. Sladjana Skopelja-Gardner JA, Joyce Tai, Lena Tanaka, Xizhang Sun, Payton Hermanson, Masaoki Kawasumi, Richard Green, Michael Gale Jr., Andrea Kalus, Victoria P. Werth, Keith B. Elkon. The early local and systemic Type I interferon responses to ultraviolet B light exposure are cGAS dependent. bioRxiv. 2019; 835132.
21. Sontheimer C, Liggitt D, Elkon KB. Ultraviolet B Irradiation Causes Stimulator of Interferon Genes-Dependent Production of Protective Type I Interferon in Mouse Skin by Recruited Inflammatory Monocytes. Arthritis Rheumatol. 2017;69(4):826-36.
22. Jefferies CA. Antiviral TRIMs: friend or foe in autoimmune and autoinflammatory disease? Clin Dev Immunol. 2011;11(9):617-25.
23. Arimoto KI, Miyauchi S, Stoner SA, Fan JB, Zhang DE. Negative regulation of type I IFN signaling. J Leukoc Biol. 2018.
24. Higgs R, Lazzari E, Wynne C, Ni Gabhann J, Espinosa A, Wahren-Herlenius M, Jefferies CA. Self protection from anti-viral responses--Ro52 promotes degradation of the transcription factor IRF7 downstream of the viral Toll-Like receptors. PLoS One. 2010;5(7):e11776.
25. Higgs R, Ni Gabhann J, Ben Larbi N, Breen EP, Fitzgerald KA, Jefferies CA. The E3 ubiquitin ligase Ro52 negatively regulates IFN-beta production post-pathogen recognition by polyubiquitin-mediated degradation of IRF3. J Immunol. 2008;181(3):1780-6.
26. Lazzari E, Korczeniewska J, Ni Gabhann J, Smith S, Barnes BJ, Jefferies CA. TRIpartite motif 21 (TRIM21) differentially regulates the stability of interferon regulatory factor 5 (IRF5) isoforms. PLoS One. 2014;9(8):e103609.

27. Espinosa A, Dardalhon V, Brauner S, Ambrosi A, Higgs R, Quintana FJ, et al. Loss of the lupus autoantigen Ro52/Trim21 induces tissue inflammation and systemic autoimmunity by disregulating the IL-23-Th17 pathway. J Exp Med. 2009;206(8):1661-71.
28. Yang B, Wang J, Sun B. Trim21: a novel negative regulator in DNA sensor signaling. Cell Mol Immunol. 2013;10(3):190-2.
29. Yoshimi R, Ishigatsubo Y, Ozato K. Autoantigen TRIM21/Ro52 as a Possible Target for Treatment of Systemic Lupus Erythematosus. Int J Rheumatol. 2012;2012:718237.
30. Zhang Z, Bao M, Lu N, Weng L, Yuan B, Liu YJ. The E3 ubiquitin ligase TRIM21 negatively regulates the innate immune response to intracellular double-stranded DNA. Nat Immunol. 2013;14(2):172-8.
31. Toda G, Yamauchi T, Kadowaki T, Ueki K. Preparation and culture of bone marrow-derived macrophages from mice for functional analysis. STAR Protoc. 2021;2(1):100246.
32. Khan M, Gasser S. Generating Primary Fibroblast Cultures from Mouse Ear and Tail Tissues. J Vis Exp. 2016(107).
33. Mazzalupo S, Wawersik MJ, Coulombe PA. An ex vivo assay to assess the potential of skin keratinocytes for wound epithelialization. J Invest Dermatol. 2002;118(5):866-70.
34. Gehrke N, Mertens C, Zillinger T, Wenzel J, Bald T, Zahn S, et al. Oxidative damage of DNA confers resistance to cytosolic nuclease TREX1 degradation and potentiates STING-dependent immune sensing. Immunity. 2013;39(3):482-95.
35. Skopelja-Gardner S, Tai J, Sun X, Tanaka L, Kuchenbecker JA, Snyder JM, et al. Acute skin exposure to ultraviolet light triggers neutrophil-mediated kidney inflammation. Proc Natl Acad Sci U S A. 2021;118(3).
36. Skopelja-Gardner S, An J, Tai J, Tanaka L, Sun X, Hermanson P, et al. The early local and systemic Type I interferon responses to ultraviolet B light exposure are cGAS dependent. Scientific reports. 2020;10(1):7908.
37. Haag SM, Gulen MF, Reymond L, Gibelin A, Abrami L, Decout A, et al. Targeting STING with covalent small-molecule inhibitors. Nature. 2018;559(7713):269-73.
38. Meller S, Winterberg F, Gilliet M, Muller A, Lauceviciute I, Rieker J, et al. Ultraviolet radiation-induced injury, chemokines, and leukocyte recruitment: An amplification cycle triggering cutaneous lupus erythematosus. Arthritis Rheum. 2005;52(5):1504-16.
39. Foering K, Chang AY, Piette EW, Cucchiara A, Okawa J, Werth VP. Characterization of clinical photosensitivity in cutaneous lupus erythematosus. J Am Acad Dermatol. 2013;69(2):205-13.
40. Boring L, Gosling J, Chensue SW, Kunkel SL, Farese RV, Jr., Broxmeyer HE, Charo IF. Impaired monocyte migration and reduced type 1 (Th1) cytokine responses in C-C chemokine receptor 2 knockout mice. J Clin Invest. 1997;100(10):2552-61.
41. Gomez-Banuelos E, Wahadat MJ, Li J, Paz M, Antiochos B, Celia AI, et al. Alternative exon usage in TRIM21 determines the antigenicity of Ro52/TRIM21 in systemic lupus erythematosus. JCI Insight. 2022;7(19).

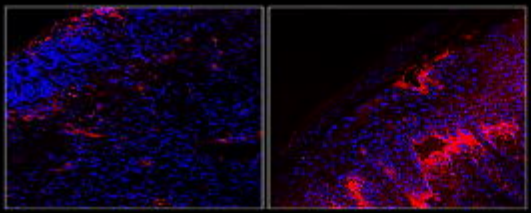

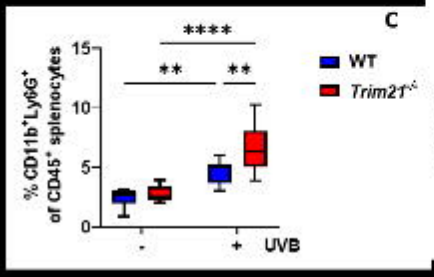
C
****
**
**
15
10
5
0
% CD11b+Ly6G+
of CD45+ splenocytes
-
+
UVB
WT
Trim21-/-

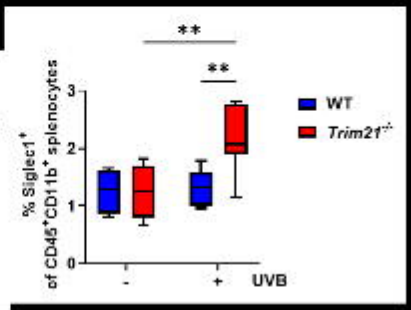
**
**
3
2
1
0
% Siglec1+
of CD45+CD11b+ splenocytes
-
+
UVB
WT
Trim21-/-

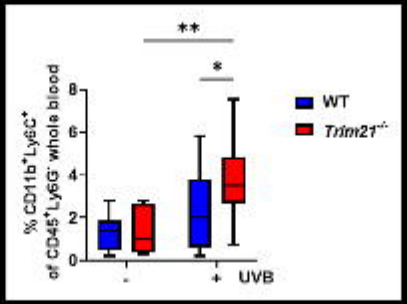
**
*
% CD11b+Ly6C+ of CD45+Ly6G- whole blood
8
6
4
2
0
-
+
UVB
WT
Trim21-/-

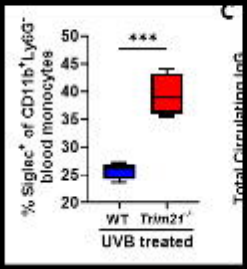
***
% Siglec+ of CD11b+Ly6G- blood monocytes
50
45
40
35
30
25
20
WT
Trim21-/-
UVB treated

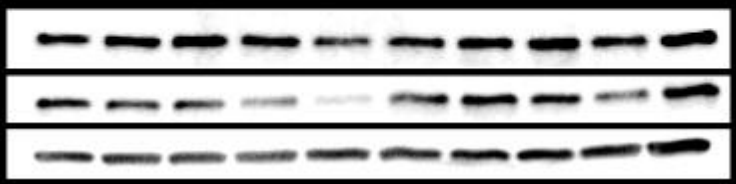

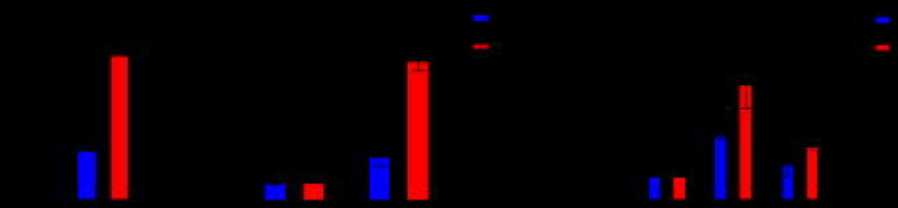

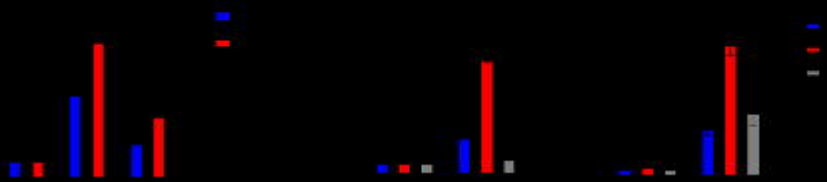

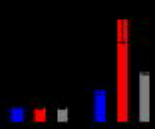

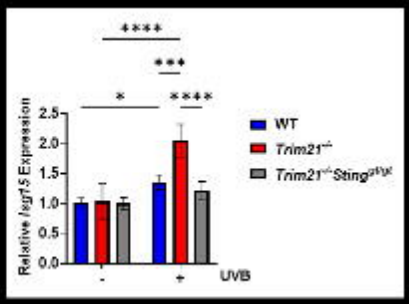
****
***
*
****
Relative Isg15 Expression
2.5
2.0
1.5
1.0
0.5
0.0
-
+
UVB
WT
Trim21-/-
Trim21-/-Sting